

TWO NONEQUIVALENT STRUCTURES FOR WIDELY-LINEAR DECISION-FEEDBACK MMSE EQUALIZATION OVER MIMO CHANNELS

Fabio Sterle, Davide Mattered and Luigi Paura

Dipartimento di Ingegneria Elettronica e delle Telecomunicazioni, Università degli Studi di Napoli Federico II
Via Claudio 21, I-80125, Napoli, Italy
phone: 0817683810, fax: +390817683149, {mattered,paura,fsterle}@unina.it
web: www.die.unina.it

ABSTRACT

The paper deals with the design of the equalizer based on the widely linear processing combined with the decision-feedback (DF) procedure and operating over time-dispersive multiple-input multiple-output channel. A basic issue concerns the choice between two widely-linear/widely-linear decision-feedback structures: the former is based on the complex-valued signal representation, whereas the latter utilizes the real-valued representation of the involved signals. Indeed, in previous contributions, both structures have been indifferently used since, in the considered scenarios, they resulted to be equivalent. In this paper, we recognize that there is an important scenario where the above structures are not equivalent. To fairly compare them, the issue of decision-error propagation has been addressed. An extensive set of experimental results shows that the real-valued signal representation-based equalizer outperforms significantly the complex-valued representation-based equalizer as well as the conventional DF equalizer when the effects of decision errors in the feedback filters are taken into account.

1. INTRODUCTION

Very recently, due to the advances in wireless communication systems, aimed at satisfying the increasing demand of high bit-rate services, much attention has been focused on multiple-input multiple-output (MIMO) communication channel models. Since the optimum (in the Maximum Likelihood sense) receiver for MIMO channel mainly suffers from the computational complexity, many suboptimal receiver structures have been proposed in order to achieve an acceptable compromise between performance and computational complexity. In the class of nonlinear symbol-by-symbol equalizers, the decision-feedback (DF) ones, which employ unlike the linear ones (referred in the following to as feedforward-based equalizers) also a linear feedback filter operating on the past decisions, have been extensively considered. It has been shown that DF strategy allows one to achieve significant performance improvements over linear equalizers both in single-input single-output [1] and in MIMO [2] scenarios. Very recently, the widely linear (WL) filtering [3] and DF equalization have been combined together to obtain the widely-linear/widely-linear decision-feedback (WL-WDF) equalizer [4] (which utilizes widely-linear processing both in feedforward filtering and in feedback filtering). Such equalizers provide significant performance advantages over both DF and WL feedforward-based equalizers. For these reasons, WL processing and DF strategy have been combined [5] in presence of dispersive MIMO channels. The equalization structures were synthesized according to the minimum mean-square error (MMSE) criterion and finite-impulse-response (FIR) filters were utilized.

As shown in [5], two alternative choices are possible to synthesize the WL receiver. The former (referred to in the sequel as real-valued representation-based equalizer (RBE))

performs the linear processing of both the real and the imaginary parts of the input vector [5, 6]. The latter (referred to in the sequel as complex-valued RBE) performs the linear processing of the input vector and its conjugate version [3]. Two important scenarios are considered in the DF equalization [2]: in the former, say Scenario 1, the estimate of the transmitted symbol block is based only on the decisions about the symbol blocks previously transmitted. In the latter, say Scenario 2, since the decisions are taken sequentially, each component of a symbol block is estimated by resorting to previous decisions about the components of the same symbol block as well as previously transmitted symbol blocks. It is easy to show [5] that real-valued and complex-valued RBEs are equivalent in Scenario 1.

In this paper, we show that in the Scenario 2 the real-valued and the complex-valued RBE structures are not equivalent anymore. To carry out a meaningful performance comparison, the optimum structures optimized also over the decision ordering have been considered and the effects of the error propagation have been considered.

The outline of the paper is the following: Section 2 introduces the WL transformation according to both the complex-valued and the real-valued representation of the signals. Section 3 presents the problem settings and the derivation of the WL-WDF-MMSE equalizer. Furthermore, Section 4 reports the results of the experiments, mainly aimed at comparing the performances of the DF equalizer and of the real-valued and the complex-valued representation-based WL-WDF equalizers. Finally, Section 5 provides the conclusions and final remarks.

2. PRELIMINARY DEFINITIONS AND BASIC PROPERTIES

In this section we first introduce some mathematical operators and representations that will be utilized in the following. Since the WL processing can be performed both by adopting the real-valued representation and the complex-valued one, operators and representations are defined for both complex and real cases. We address the problem of finding the main correspondences and differences between the WL transformations for both the complex case and the real one.

2.1 Preliminary definitions

Let us define the following operators:

$$\tilde{\mathcal{C}}_p[\mathbf{u}] \triangleq \begin{bmatrix} \mathbf{u}(1 : n_1, 1 : p) & \mathbf{u}(1 : n_1, p + 1 : n_2) \\ \mathbf{u}^*(1 : n_1, 1 : p) & \mathbf{0}_{n_1 \times (n_2 - p)} \\ \mathbf{0}_{n_1 \times (n_2 - p)} & \mathbf{u}^*(1 : n_1, p + 1 : n_2) \end{bmatrix} \quad (1)$$

$$\tilde{\mathcal{E}}_p[\mathbf{u}] \triangleq \begin{bmatrix} \Re\{\mathbf{u}(1:n_1, 1:p)\} & \Re\{\mathbf{u}(1:n_1, p+1:n_2)\} \\ \Im\{\mathbf{u}(1:n_1, 1:p)\} & \Im\{\mathbf{u}(1:n_1, p+1:n_2)\} \\ -\Im\{\mathbf{u}(1:n_1, p+1:n_2)\} & \Re\{\mathbf{u}(1:n_1, p+1:n_2)\} \end{bmatrix} \quad (2)$$

$$\mathcal{C}_p[\mathbf{u}] \triangleq \begin{bmatrix} \mathbf{u} \\ \mathbf{u}^*(p+1:n_1, 1:n_2) \end{bmatrix} \quad (3)$$

$$\mathcal{E}_p[\mathbf{u}] \triangleq \begin{bmatrix} \Re\{\mathbf{u}\} \\ \Im\{\mathbf{u}(p+1:n_1, 1:n_2)\} \end{bmatrix} \quad (4)$$

where $\mathbf{u} \in \mathbb{C}^{n_1 \times n_2}$, $0 \leq p \leq n_1$ is an integer value, $\mathbf{u}(i_1 : \ell_1, i_2 : \ell_2)$ is the submatrix of \mathbf{u} , whose first and last rows (columns) are the i_1 th (i_2 th) and the ℓ_1 th (ℓ_2 th) ones, respectively, $\Re\{\cdot\}$ and $\Im\{\cdot\}$ denote real and the imaginary part, the superscript $*$ denotes the complex conjugation, and, finally, the array $\mathbf{0}_{n_1 \times n_2}$ is the $n_1 \times n_2$ matrix containing all null entries (the specification of the size $n_1 \times n_2$ will be omitted in the sequel for the sake of brevity). The operators (1)-(4), as it will be shown in Section 3, allow us to rewrite the input-output relation of a MIMO linear (time-dispersive) channel so that the WL-WDF equalizer can be synthesized by utilizing the procedure relative to the DF equalization of [2]. Moreover, the operators (4) are utilized to describe the basic properties of the WL transformations introduced in the next subsection.

Let us also define the operators

$$\bar{\mathcal{C}}_p \begin{bmatrix} \mathbf{u}_1 \\ \mathbf{u}_2 \end{bmatrix} = \mathbf{u}_1 \quad \bar{\mathcal{E}}_p \begin{bmatrix} \mathbf{u}_3 \\ \mathbf{u}_4 \\ \mathbf{u}_5 \end{bmatrix} = \begin{bmatrix} \mathbf{u}_3 \\ \mathbf{u}_4 + j\mathbf{u}_5 \end{bmatrix}$$

where j is the imaginary unit, \mathbf{u}_1 has n_1 rows, \mathbf{u}_2 , \mathbf{u}_4 , \mathbf{u}_5 has $n_1 - p$ rows and \mathbf{u}_3 have p rows. The operators $\bar{\mathcal{C}}_p[\cdot]$ and $\bar{\mathcal{E}}_p[\cdot]$ represent the inverse of $\mathcal{C}_p[\cdot]$ and $\mathcal{E}_p[\cdot]$, respectively. The parameter p denotes the number of real-valued components of the input vector \mathbf{u} . Therefore, when the first p components of \mathbf{u} are real-valued, then $\bar{\mathcal{C}}_p[\mathcal{C}_p[\mathbf{u}]] = \mathbf{u}$ and $\bar{\mathcal{E}}_p[\mathcal{E}_p[\mathbf{u}]] = \mathbf{u}$. Finally, similarly to [7], let us define the matrix transformation

$$\mathbf{T} \triangleq \begin{bmatrix} \mathbf{I}_p & \mathbf{0} & \mathbf{0} \\ \mathbf{0} & \mathbf{I}_{n_1-p} & j\mathbf{I}_{n_1-p} \\ \mathbf{0} & \mathbf{I}_{n_1-p} & -j\mathbf{I}_{n_1-p} \end{bmatrix}, \quad \mathbf{T}\mathbf{T}^H = \mathbf{T}^H\mathbf{T} = \mathbf{I}_{2n_1-p} \quad (6)$$

If \mathbf{u} is a vector with n_1 rows such that the first p rows are real-valued, then $\mathcal{C}_p[\mathbf{u}] = \mathbf{T}\mathcal{E}_p[\mathbf{u}]$.

2.2 Widely Linear Transformations

By adopting the real-valued representation, the WL transformation from \mathbf{x} to \mathbf{y} is defined as the linear transformation on the extended vector $\mathcal{E}_{n_r}[\mathbf{x}]$, namely:

$$\mathcal{E}_{n_q}[\mathbf{y}] \triangleq \begin{bmatrix} \mathbf{F}_{11} & \mathbf{F}_{12} & \mathbf{F}_{13} \\ \mathbf{F}_{21} & \mathbf{F}_{22} & \mathbf{F}_{23} \\ \mathbf{F}_{31} & \mathbf{F}_{32} & \mathbf{F}_{33} \end{bmatrix} \mathcal{E}_{n_r}[\mathbf{x}] = \mathbf{F}\mathcal{E}_{n_r}[\mathbf{x}]. \quad (7)$$

where the first n_q components of \mathbf{y} are real-valued, $\mathbf{F}_{11} \in \mathbb{R}^{n_q \times n_r}$, $\mathbf{F}_{12}, \mathbf{F}_{13} \in \mathbb{R}^{n_q \times (n_i - n_r)}$, $\mathbf{F}_{21}, \mathbf{F}_{31} \in \mathbb{R}^{(n_o - n_q) \times n_r}$, and where $\mathbf{F}_{\ell k} \in \mathbb{R}^{(n_o - n_q) \times (n_i - n_r)}$ with $\ell, k = 2, 3$. More specifically, the widely linear transformation from \mathbf{x} to \mathbf{y} can be written as: $\mathbf{y} = \bar{\mathcal{E}}_{n_q}[\mathbf{F}\mathcal{E}_{n_r}[\mathbf{x}]]$.

The linear transformation (7) can also be equivalently written as:

$$\mathcal{C}_{n_q}[\mathbf{y}] \triangleq \begin{bmatrix} \mathbf{G}_{11} & \mathbf{G}_{12} & \mathbf{G}_{12}^* \\ \mathbf{G}_{21} & \mathbf{G}_{22} & \mathbf{G}_{23} \\ \mathbf{G}_{21}^* & \mathbf{G}_{23}^* & \mathbf{G}_{22}^* \end{bmatrix} \mathcal{C}_{n_r}[\mathbf{x}] = \mathbf{G}\mathcal{C}_{n_r}[\mathbf{x}] \quad (8)$$

where

$$\mathbf{G} = \mathbf{T}\mathbf{F}\mathbf{T}^H. \quad (9)$$

Then, the overall WL processing can also be written as: $\mathbf{y} = \bar{\mathcal{C}}_{n_q}[\mathbf{G}\mathcal{C}_{n_r}[\mathbf{x}]]$. In other words, when a matrix \mathbf{F} for WL processing in real-valued representation is available, then the matrix for the corresponding WL processing in complex-valued representation is $\mathbf{G} = \mathbf{T}\mathbf{F}\mathbf{T}^H$ and, *vice versa*, $\mathbf{F} = \mathbf{T}^H\mathbf{G}\mathbf{T}$ is the relation for the inverse transformation between the two representations.

In the literature [3-5], the two representations are both used since they are often equivalent for many application scenarios. However, it can be verified that such an equivalence does not hold in general. Let us further discuss how it may happen that the choice of the representation implies a difference in the performances. Let us denote with $S_r^{(1)}$ and $S_r^{(2)}$ two sets of matrices \mathbf{F} in the real-valued representation corresponding, by means of the transformation (9), to the sets $S_c^{(1)}$ and $S_c^{(2)}$ of matrices \mathbf{G} in the complex-valued representation, respectively. Assume that $S_r^{(1)}$ satisfies a constraint on the structure of its elements, and $S_c^{(2)}$ satisfies a constraint on the structure of its elements. Then, if $S_r^{(1)} \neq S_r^{(2)}$ and, therefore, $S_c^{(1)} \neq S_c^{(2)}$, the two representations are not equivalent. In fact, the choice of the real-valued representation means to search for the matrix \mathbf{F} in $S_r^{(1)}$, while choosing the complex-valued representation is equivalent to search for the matrix \mathbf{F} in $S_r^{(2)}$; the two representations are equivalent only in the special case where the chosen matrices in $S_r^{(1)}$ and $S_r^{(2)}$ belong to the intersection of $S_r^{(1)}$ and $S_r^{(2)}$. In other words, choosing the complex-valued representation means to search for the matrix \mathbf{G} in $S_c^{(2)}$, while choosing the real-valued representation is equivalent to search for the matrix \mathbf{G} in $S_c^{(1)}$. An important example is provided by the WL-WDF-MMSE equalization in Scenario 2 where, as it will be shown in Section 3, a lower triangular structure is imposed on the matrix filter. More specifically, a lower-triangular matrix $\mathbf{F} \in S_r^{(1)}$ needs to be utilized when the real-valued representation is adopted, while a lower-triangular matrix $\mathbf{G} \in S_c^{(2)}$ needs to be utilized when the complex-valued representation is chosen. Since the set $S_c^{(1)}$ corresponding to $S_r^{(1)}$ by means of the transformation (9) is different from $S_c^{(2)}$, the choice of the two representations leads to the optimization over two different sets and, hence, in general different optimum solutions are obtained in correspondence of the two possible choices.

3. MIMO INPUT-OUTPUT MODEL AND IDEAL WL-WDF-MMSE EQUALIZATION

Let us consider a FIR baseband equivalent noisy communication channel with n_i jointly wide-sense stationary (WSS) transmitted signals and n_o received signals. The inputs and the outputs of the MIMO channel at the k th instant are $\mathbf{x}_k = [x_k^{(1)} \ x_k^{(2)} \ \dots \ x_k^{(n_i)}]^T$ and $\mathbf{y}_k = [y_k^{(1)} \ y_k^{(2)} \ \dots \ y_k^{(n_o)}]^T$. Using a matrix representation, the output vector \mathbf{y}_k can be expressed as follows:

$$\mathbf{y}_k = \sum_{m=0}^{\nu} \mathbf{H}_m \mathbf{x}_{k-m} + \mathbf{n}_k \quad (10)$$

where ν denotes the channel order, \mathbf{H}_m is the $n_o \times n_i$ matrix whose entry $h_m^{(i,\ell)}$ accounts for the effect of the ℓ th input on the i th output, and \mathbf{n}_k is the $n_o \times 1$ vector of noise samples at the k th instant. Each symbol $x_k^{(i)}$ is drawn from the constellations S_i ($i = 1, \dots, n_i$): with no loss of generality, we consider both the complex-valued constellations (e.g., MPSK with $M \geq 4$ and QAM) and real-valued constellation (e.g., PAM) as in [5], and we assume unit-power symbol sequences $x_k^{(i)}$. We order the symbol sequences so that the real-valued

$$\begin{bmatrix} \mathbf{C}_0[\mathbf{y}_k] \\ \mathbf{C}_0[\mathbf{y}_{k-1}] \\ \mathbf{C}_0[\mathbf{y}_{k-(N_f-1)}] \end{bmatrix} = \begin{bmatrix} \tilde{\mathbf{C}}_{n_r}^P[\mathbf{H}_0] & \dots & \tilde{\mathbf{C}}_{n_r}^P[\mathbf{H}_\nu] & \mathbf{0} & \dots & \mathbf{0} \\ \mathbf{0} & \tilde{\mathbf{C}}_{n_r}^P[\mathbf{H}_0] & \dots & \tilde{\mathbf{C}}_{n_r}^P[\mathbf{H}_\nu] & \mathbf{0} & \vdots \\ \vdots & \vdots & \ddots & \ddots & \vdots & \vdots \\ \mathbf{0} & \dots & \mathbf{0} & \tilde{\mathbf{C}}_{n_r}^P[\mathbf{H}_0] & \dots & \tilde{\mathbf{C}}_{n_r}^P[\mathbf{H}_\nu] \end{bmatrix} \cdot \begin{bmatrix} \mathbf{C}_{n_r}[\mathbf{x}_k] \\ \mathbf{C}_{n_r}[\mathbf{x}_{k-1}] \\ \mathbf{C}_{n_r}[\mathbf{x}_{k-(N_f+\nu-1)}] \end{bmatrix} + \begin{bmatrix} \mathbf{C}_0[\mathbf{n}_k] \\ \mathbf{C}_0[\mathbf{n}_{k-1}] \\ \mathbf{C}_0[\mathbf{n}_{k-(N_f-1)}] \end{bmatrix} \quad (13)$$

constellations have indices $i \in \{1, \dots, n_r\}$. By resorting to the transformations (1) and (4), the channel model (10) can be replaced by the following equivalent one:

$$\mathbf{C}_0[\mathbf{y}_k] = \sum_{m=0}^{\nu} \tilde{\mathbf{C}}_{n_r}^P[\mathbf{H}_m] \mathbf{C}_{n_r}[\mathbf{x}_{k-m}] + \mathbf{C}_0[\mathbf{n}_k]. \quad (11)$$

Let \mathbf{P} be a permutation matrix of size $2n_i - n_r$, such that $\mathbf{P}^T \mathbf{P} = \mathbf{I}_{2n_i - n_r}$. By defining the (row) permuted input vector $\mathbf{C}_{n_r}^P[\mathbf{x}_k] \triangleq \mathbf{P} \mathbf{C}_{n_r}[\mathbf{x}_k]$ and, hence, the (column) permuted channel matrix $\tilde{\mathbf{C}}_{n_r}^P[\mathbf{H}_m] \triangleq \tilde{\mathbf{C}}_{n_r}[\mathbf{H}_m] \mathbf{P}^T$, the channel output can be equivalently re-written as follows:

$$\mathbf{C}_0[\mathbf{y}_k] = \sum_{m=0}^{\nu} \tilde{\mathbf{C}}_{n_r}^P[\mathbf{H}_m] \mathbf{C}_{n_r}^P[\mathbf{x}_{k-m}] + \mathbf{C}_0[\mathbf{n}_k]. \quad (12)$$

Since we consider FIR equalizers, it is useful to express (12) in matrix representation; specifically, by considering a block of N_f received vectors $\mathbf{C}_0[\mathbf{y}_k]$, (12) can be re-written as in (13), or, more compactly,

$$\tilde{\mathbf{y}}_k = \tilde{\mathbf{H}}(P) \tilde{\mathbf{x}}_k(P) + \tilde{\mathbf{n}}_k. \quad (14)$$

With reference to channel model (14), we define the input-correlation matrix of size $(N_f + \nu)(2n_i - n_r)$

$$\mathbf{R}_{\tilde{\mathbf{x}}}(P) \triangleq E \left[\tilde{\mathbf{x}}_k(P) \tilde{\mathbf{x}}_k^H(P) \right] \quad (15)$$

and the noise-correlation matrix of size $2n_o N_f$

$$\mathbf{R}_{\tilde{\mathbf{n}}} \triangleq E \left[\tilde{\mathbf{n}}_k \tilde{\mathbf{n}}_k^H \right]. \quad (16)$$

It follows that the input-output cross-correlation matrix and the output-correlation matrix are given by

$$\mathbf{R}_{\tilde{\mathbf{y}}\tilde{\mathbf{x}}}(P) \triangleq E \left[\tilde{\mathbf{y}}_k \tilde{\mathbf{x}}_k^H(P) \right] = \tilde{\mathbf{H}}(P) \mathbf{R}_{\tilde{\mathbf{x}}}(P) \quad (17)$$

$$\mathbf{R}_{\tilde{\mathbf{y}}} \triangleq E \left[\tilde{\mathbf{y}}_k \tilde{\mathbf{y}}_k^H \right] = \tilde{\mathbf{H}} \mathbf{R}_{\tilde{\mathbf{x}}} \tilde{\mathbf{H}}^H + \mathbf{R}_{\tilde{\mathbf{n}}} \quad (18)$$

where we have taken into account that the channel output \mathbf{y}_k and $\tilde{\mathbf{y}}_k$ (and, therefore, also its second-order statistics) are independent of \mathbf{P} .

The output, say $\mathbf{z}_{k-\Delta}(P)$, of the WL-WDF equalizer is obtained by applying the transformation $\tilde{\mathbf{C}}_{n_r}^P[\cdot]$ to the output $\mathbf{z}_{\mathbf{C},k-\Delta}(P)$ of the DF equalizer operating on the channel (12), i.e., $\mathbf{z}_{k-\Delta}(P) = \tilde{\mathbf{C}}_{n_r}^P[\mathbf{z}_{\mathbf{C},k-\Delta}(P)]$ where

$$\begin{aligned} \mathbf{z}_{\mathbf{C},k-\Delta}(P) &\triangleq \sum_{\ell=0}^{N_f-1} \mathbf{W}_\ell^H \mathbf{C}_0[\mathbf{y}_{k-\ell}] \\ &+ \sum_{i=0}^{N_b} (\mathbf{I}_{2n_i - n_r} \delta_i - \mathbf{B}_i^H) \mathbf{P} \mathbf{C}_{n_r}[\tilde{\mathbf{x}}_{k-\Delta-i}] \end{aligned} \quad (19)$$

where \mathbf{W}_ℓ and \mathbf{B}_i denote the matrix taps of size $2n_o \times (2n_i - n_r)$ and $(2n_i - n_r) \times (2n_i - n_r)$, respectively, δ_k

is the Kronecker delta, $\tilde{\mathbf{x}}_{k-\Delta-i}$ is an estimate of $\mathbf{x}_{k-\Delta-i}$ ($i = 0, \dots, N_b$), and the integer Δ denotes a processing delay. Note that each permutation matrix \mathbf{P} defines a different decision ordering and, so, a different DF equalizer. The feedforward filter matrix $\mathbf{W}_{\mathbf{C}} \triangleq [\mathbf{W}_0^H \ \mathbf{W}_1^H \ \dots \ \mathbf{W}_{N_f-1}^H]^H$ and the feedback one $\mathbf{B}_{\mathbf{C}} \triangleq [\mathbf{B}_0^H \ \mathbf{B}_1^H \ \dots \ \mathbf{B}_{N_b}^H]^H$ are chosen according to the MMSE criterion, i.e.,

$$\min_{\mathbf{W}_{\mathbf{C}}, \mathbf{B}_{\mathbf{C}}} E \left[\|\mathbf{e}_{k-\Delta}(P)\|^2 \right] \quad (20)$$

$$\mathbf{e}_{k-\Delta}(P) \triangleq \mathbf{z}_{\mathbf{C},k-\Delta}(P) - \mathbf{C}_{n_r}^P[\mathbf{x}_{k-\Delta}]$$

with $\mathbf{e}_{k-\Delta}(P)$ denoting the error vector, with correlation matrix defined as $\mathbf{R}_{\mathbf{e}}(P) \triangleq E \left[\mathbf{e}_{k-\Delta}(P) \mathbf{e}_{k-\Delta}^H(P) \right]$. The ‘‘ideal WL-WDF-MMSE equalizer’’ is obtained by performing the minimization (20) under the assumption that past decisions are correct. By utilizing the results in [1], it can be shown that the optimum feedforward filter $\mathbf{W}_{\mathbf{C}}^{(opt)}$ is given by

$$\mathbf{W}_{\mathbf{C}}^{(opt)}(P) = \mathbf{R}_{\tilde{\mathbf{y}}\tilde{\mathbf{x}}}^{-1} \mathbf{R}_{\tilde{\mathbf{y}}\tilde{\mathbf{x}}}(P) \Psi_{\Delta} \mathbf{B}_{\mathbf{C}}(P) \quad (21)$$

with

$$\Psi_{\Delta} \triangleq \begin{bmatrix} \mathbf{0}_{\Delta(2n_i - n_r) \times (2n_i - n_r)(N_b+1)} \\ \mathbf{I}_{(2n_i - n_r)(N_b+1)} \\ \mathbf{0}_{s(2n_i - n_r) \times (2n_i - n_r)(N_b+1)} \end{bmatrix}.$$

The optimization problem (20) can be solved assuming that *i*) only past decisions are available for estimating $\mathbf{C}_{n_r}[\mathbf{x}_{k-\Delta}]$ (say Scenario 1); *ii*) past decisions and current decisions with lower indexed components are available for estimating $\mathbf{C}_{n_r}[\mathbf{x}_{k-\Delta}]$ (say Scenario 2). These two scenarios are mathematically described by constraints introduced on the matrix tap \mathbf{B}_0 . Specifically, the condition $\mathbf{B}_0 = \mathbf{I}_{2n_i - n_r}$ holds when Scenario 1 is considered, while \mathbf{B}_0 is constrained to be upper triangular with unit diagonal entries (monic) when Scenario 2 is considered. It can be shown that the optimum feedback filters and the corresponding MSE are:

$$\begin{aligned} &\text{Scenario 1} \\ \mathbf{B}_{\mathbf{C},1}^{(opt)}(P) &= (\mathbf{R}_{\Delta}(P))^{-1} \Phi \left[\Phi^H (\mathbf{R}_{\Delta}(P))^{-1} \Phi \right]^{-1} \\ \text{MMSE}_1(P) &= \text{trace} \left(\left[\Phi^H (\mathbf{R}_{\Delta}(P))^{-1} \Phi \right]^{-1} \right) \end{aligned} \quad (22)$$

$$\begin{aligned} &\text{Scenario 2} \\ \mathbf{B}_{\mathbf{C},2}^{(opt)}(P) &= \mathbf{B}_{\mathbf{C},1}^{(opt)}(P) \mathbf{B}_0^{(opt)}(P) \\ \left[\Phi^H (\mathbf{R}_{\Delta}(P))^{-1} \Phi \right]^{-1} &= \mathbf{L}(P) \mathbf{D}(P) \mathbf{L}(P)^H \\ \mathbf{B}_0^{(opt)}(P) &= \mathbf{L}(P)^{-H} \\ \text{MMSE}_2(P) &= \text{trace}(\mathbf{D}(P)) \end{aligned} \quad (23)$$

where $\Phi \triangleq [\mathbf{I}_{2n_i - n_r} \ \mathbf{0}_{(2n_i - n_r) \times N_b(2n_i - n_r)}]^H$ and the matrices $\mathbf{L}(P)$ and $\mathbf{D}(P)$ are obtained by performing the Cholesky factorization of the matrix $[\Phi^H (\mathbf{R}_{\Delta}(P))^{-1} \Phi]^{-1}$. By resorting to the property $\text{trace}(\mathbf{A}) = \text{trace}(\mathbf{X}^{-1} \mathbf{A} \mathbf{X})$, with \mathbf{X} being a unitary matrix, it can be verified that $\text{MMSE}_1(P) = \text{MMSE}_1(\mathbf{I}) \forall \mathbf{P}$, i.e., the performances of DF-based equalizers are invariant to the decision ordering when Scenario 1 is

considered. On the other hand, if Scenario 2 is considered, the permutation matrix \mathbf{P} greatly affects the MMSE (20) achieved by DF-based equalizers and, therefore, $(2n_i - n_r)!$ different WL-WDF equalizers exist. Unfortunately, the optimum decision ordering can be derived only by an exhaustive procedure.

Non-equivalent structures

According to the real-valued representation, the channel model (11) can be equivalently rewritten [5] as

$$\mathcal{E}_0[\mathbf{y}_k] = \sum_{m=0}^{\nu} \tilde{\mathcal{E}}_{n_r}[\mathbf{H}_m] \mathcal{E}_{n_r}[\mathbf{x}_{k-m}] + \mathcal{E}_0[\mathbf{n}_k]. \quad (24)$$

The DF equalizer operating on such a channel model defines the WL-WDF equalizer structure according to the real-valued representation. It is simple to verify that the framework utilized to derive the WL-WDF-MMSE according to the complex-valued representation allows one to derive the WL-WDF-MMSE according to the real-valued representation. In [5], it has been shown that a one-to-one correspondence exists between such a representation and the complex-valued one when Scenario 1 is considered. On the other hand, let us note that, due to the constraint imposed by the Scenario 2, the matrix tap $\mathbf{B}_0^{(opt)}(P)$ is monic upper triangular, and hence, on the basis of the results in Section 2.2, the complex-valued equalizer structure and the real-valued one are not equivalent.

4. PERFORMANCE ANALYSIS OF THE PROPOSED EQUALIZERS

In this section, we present the results of computer simulations carried out to assess the performances of the different equalizers considered in the previous section. We first consider in subsection 4.1 the case where no error propagation is present. Then, in subsection 4.2, we consider the case where the effects of error propagation in DF equalization are taken into account. The equalizer performances have been optimized over all the decision orderings by an exhaustive procedure.

4.1 Ideal Decision-Feedback Results

In this subsection we present the performances of the ideal WL-WDF-MMSE equalizers. The performances are evaluated in terms of signal-to-noise ratio (SNR) at the decision point defined as

$$\text{SNR} \triangleq \left(\frac{1}{n_i} E \left[\|\bar{\mathcal{C}}_{n_r}[\mathbf{z}_{c,k-\Delta}(P)] - \mathbf{x}_{k-\Delta}\|^2 \right] \right)^{-1}$$

and optimized with respect to Δ . Moreover, the optimum feedback filter memory $N_b = N_f + \nu - \Delta - 1$ has been chosen. The averaged SNR (ASNR) in dB is obtained by averaging the obtained results over 100 independent trials: in each trial, the channel taps $h_m^{(i,\ell)}$ ($i = 1, \dots, n_i$, $\ell = 1, \dots, n_o$) are randomly generated according to a complex zero-mean white Gaussian random process with unitary variance and uncorrelated with each other. Unless not specified, in the following simulations, we assume $n_i = 4$ spatially and temporally uncorrelated unit power input sequences, $n_r = 2$, $n_c = n_i - n_r$ complex-valued circularly symmetric input sequences, n_o complex-valued white WSS Gaussian zero-mean noise sequences with the same power σ_n^2 , $\nu = 1$, and $N_f = 4$. Moreover, we denote the WL-WDF-MMSE equalizer obtained by adopting the complex-valued representation with WLWDF-C, while WLWDF-R will denote the WL-WDF-MMSE equalizer obtained by adopting the real-valued representation. The two Scenarios (22) and (23) are denoted with the abbreviations Sc.1 and Sc.2, respectively.

We have evaluated the performance relative gain G_1 of the WLWDF-C equalizer over the WLWDF-R one, the performance relative gain G_2 of the WLWDF-R equalizer over the DF-MMSE equalizer in both Sc.1 and Sc.2, the performance relative gain G_3 of the WLWDF-R equalizer in Scenario 2 over the same equalizer in Scenario 1, and, finally, the performance relative gain G_4 of the DF equalizer in Scenario 2 over the same equalizer in Scenario 1. More specifically:

$$\begin{aligned} G_1 &\triangleq \frac{\text{ASNR}_{\text{WLWDF-C}}(\text{dB}) - \text{ASNR}_{\text{WLWDF-R}}(\text{dB})}{\min \{ \text{ASNR}_{\text{WLWDF-C}}(\text{dB}), \text{ASNR}_{\text{WLWDF-R}}(\text{dB}) \}} \\ G_2 &\triangleq \frac{\text{ASNR}_{\text{WLWDF-R}}(\text{dB}) - \text{ASNR}_{\text{DF}}(\text{dB})}{\text{ASNR}_{\text{DF}}} \\ G_3 &\triangleq \frac{\text{ASNR}_{\text{WLWDF-R}}^{(\text{Sc.2})}(\text{dB}) - \text{ASNR}_{\text{WLWDF-R}}^{(\text{Sc.1})}(\text{dB})}{\text{ASNR}_{\text{WLWDF-R}}^{(\text{Sc.1})}(\text{dB})} \\ G_4 &\triangleq \frac{\text{ASNR}_{\text{DF}}^{(\text{Sc.2})}(\text{dB}) - \text{ASNR}_{\text{DF}}^{(\text{Sc.1})}(\text{dB})}{\text{ASNR}_{\text{DF}}^{(\text{Sc.1})}(\text{dB})} \end{aligned}$$

where G_2 is evaluated for both Sc.1 and Sc.2. Figs. 1 (a)-(b) report $[G_i]_{i=1, \dots, 4}$ versus the number of channel outputs n_o for $\text{SNR}_i = 15\text{dB}$ and $\text{SNR}_i = 30\text{dB}$, respectively. Note that the WLWDF-C equalizer reaches its largest gain G_1 over the WLWDF-R equalizer for $n_o < n_i$; moreover, G_1 exhibits the maximum value for $n_o = 2$ in presence of large SNR_i . Similarly, the gain G_2 of the WLWDF-R equalizer over the DF is different from zero for $n_o < n_i$ both in Sc.1 and in Sc.2; more specifically, G_2 exhibits its maximum for $n_o = 3$ when Sc.1 is considered, while it is constant for $n_o < n_i$ when Sc.2 is considered. The performance improvement gained by the WL processing, for fixed n_i and n_o , is due to a better exploitation of the statistical redundancy exhibited by the useful signal component. As expected, similarly to G_1 , also G_2 approaches to zero when n_o increases. Finally, the gains G_3 and G_4 monotonically decrease with n_o . The feedback of current decisions (Scenario 2) allows one to achieve a large gain over the equalizer structures of the Scenario 1 when n_o is lower than n_i since they guarantee the capability to discriminate the n_i inputs.

4.2 Error propagation in WL-WDF equalization

Since the performances of the DF-based equalizers are also affected by the presence of the error propagation, in the following we analyze by computer simulations the effects of the error propagation when the WL-WDF-MMSE is employed at the receiver side. More specifically, we single out important differences between the complex-valued representation-based equalizer and the real-valued representation-based one when Scenario 2 is considered.

We consider a 2×1 MIMO channel model (Fig. 2) and a 2×2 one (Fig. 3). BPSK and 4-QAM constellations are assumed to be employed for the real-valued input sequence and the complex-valued circularly symmetric one, respectively (i.e., $n_r = 1$ and $n_c = 1$). The number of the feed-forward matrix taps is set to $N_f = 2$ and all the equalizer parameters are chosen according to the MMSE criterion. In presence of error propagation we use, as performance measure, the bit error rate (BER) averaged over the n_i inputs; moreover, the BER curves are exhaustively optimized over all the possible decision orderings and are averaged over 100 independent channel realizations. In Figs. 2 and 3 the SERs of the considered equalizers in Scenario 2 are plotted versus SNR_i both in absence and in presence of error propagation. The reported BER curves show that the WLWDF-C equalizer, which outperforms all the other equalizers when correct decisions feed the feedback filter (see the black lines), can perform very poorly (see the grey lines) in the presence of error propagation. In such a scenario the WLWDF-R equalizer outperforms all the other equalizers.

The results of such analysis are completely different from those obtained in the previous subsection where the error propagation effects were not taken into account. In fact, the WLWDF-C equalizer is able to utilize the decision over the conjugate version of $x_{k-\Delta}^{(i)}$ to improve the estimate of $x_{k-\Delta}^{(i)}$ (and *vice versa*). However, such an improvement holds only when $\hat{x}_{k-\Delta}^{(i)} = x_{k-\Delta}^{(i)}$, i.e. when the estimation error is enough small to allow to achieve a correct decision. It follows that the achieved accuracy improvement in estimating $x_{k-\Delta}^{(i)}$ (correspondent to an increase in the SNR at the decision point) does not reduce the probability of error.

5. CONCLUSIONS

The paper addresses the widely-linear decision-feedback equalization over time-dispersive MIMO channels when the receiver exploits not only past decisions, but also the available current decisions (in the paper referred to as Scenario 2) so that also the decision ordering has to be optimized. The paper shows that two non-equivalent WLWDF-MMSE equalizer structure can be obtained by resorting to the complex-valued representation of the baseband signals and to the real-valued one. The results show that real-valued representation-based structure outperforms the complex-valued representation-based one since it is more tolerant to the effects of decision errors in the feedback filter.

REFERENCES

- [1] N. Al-Dahir and J. Cioffi, "MMSE decision-feedback equalizers: Finite length results," *IEEE Trans. on Information Theory*, vol. 41, pp. 961–975, July 1995.
- [2] N. Al-Dhahir and A. H. Sayed, "The finite-length multi-input multi-output MMSE DFE," *IEEE Trans. on Signal Processing*, vol. 48, pp. 2921–2936, Oct. 2000.
- [3] B. Picinbono and P. Chevalier, "Widely linear estimation with complex data," *IEEE Trans. on Signal Processing*, vol. 43, pp. 2030–2033, Aug. 1995.
- [4] W. Gerstacker, F. Obernosterer, R. Schober, A. Lehmann, A. Lampe, and P. Gunreben, "Widely linear equalization for space-time block-coded transmission over fading ISI channels," in *Vehicular Technology Conference, 2002.-Fall*, pp. 238–242, Sept. 2002.
- [5] D. Mattera, L. Paura, and F. Sterle, "Widely linear decision-feedback equalizer for time-dispersive linear MIMO channels," *IEEE Trans. on Signal Processing*, vol. 53, pp. 2525–2536, July 2005.
- [6] M. K. Varanasi, "Multiuser detection for overloaded CDMA systems," *IEEE Trans. on Information Theory*, vol. 49, pp. 1728–1742, July 2003.
- [7] B. Picinbono, "Second-order complex random vectors and normal distributions," *IEEE Trans. on Signal Processing*, vol. 44, pp. 2637–2640, Oct. 1996.

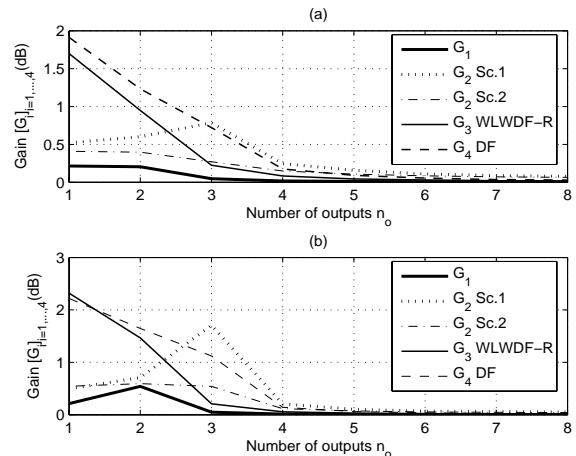


Figure 1: Gains $[G_i]_{i=1,\dots,4}$ versus the number of outputs n_o for $SNR_i = 15$ dB (a) and $SNR_i = 30$ dB (b).

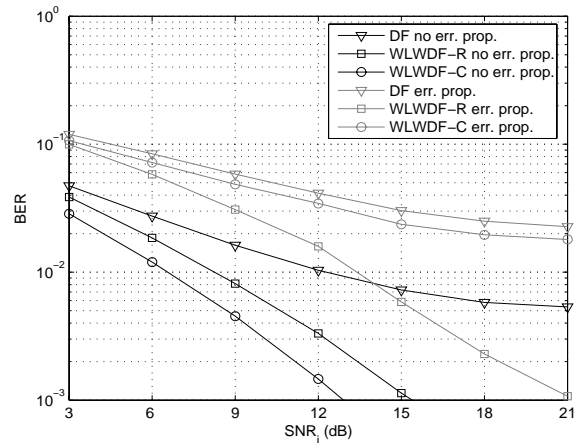


Figure 2: BERs of the equalizers versus SNR_i ; 2×1 MIMO channel.

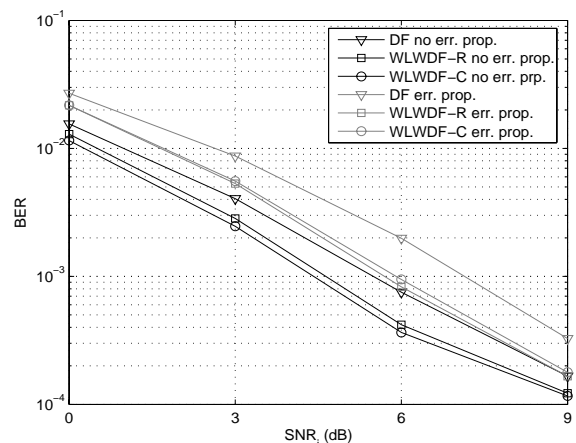


Figure 3: BERs of the equalizers versus SNR_i ; 2×2 MIMO channel.